INTERNATIONAL JOURNAL OF OPTIMIZATION IN CIVIL ENGINEERING
Int. J. Optim. Civil Eng., 2024; 14(3):423–444

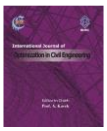

PERFORMANCE ASSESSMENT OF CONTOURLET TRANSFORM IN DAMAGE DETECTION OF PLATE STRUCTURES

A.R. Hajizadeh[1], M. Khatibinia[2,*, †], D. Hamidian[3]
[1]*Department of Civil Engineering, National University of Skills (NUS), Tehran, Iran*
[2]*Department of Civil Engineering, University of Birjand, Birjand, Iran*
[3]*Department of Civil Engineering, Islamic Azad University, Gachsaran, Iran*

ABSTRACT

The contourlet transform as an extension of the wavelet transform in two dimensions uses the multiscale and directional filter banks, and has a more adequate performance in comparison with the classical multi-scale representations. In this study, the efficiency of the contourlet transform is assessed for identifying the damage of plate structures in various conditions. The conditions include single damage and multi–damages with different shapes and severities, the different supports (i.e., boundary conditions), and the higher mode shapes,. For achieving this purpose, the process of the damage detection of plate structures using contourlet transform is implemented in the three steps. In the first step, the first mode shapes of a damaged plate and a reference state as the intact plate are obtained using the finite element method. In the second step, the damage indices are achieved by applying the contourlet transform to the responses of the first mode shapes for the damaged and intact plates. Finally, the location and the approximate shape of the damage are identified by plotting the damage indices. The obtained results indicate that the various conditions influence the performance of the contourlet transform for identifying the location and approximate shape of damages in plate structures.

Keywords: damage detection; contourlet transform; Laplacian pyramid; directional filter banks; plate structure; mode shape.

Received: 24 July 2024; Accepted: 7 September 2024

1. INTRODUCTION

The damage detection and the structural health monitoring of structural and mechanical systems have considerably attracted the attention of researchers over the last years [1–7]. Since the occurrence of damage alters the performance of structures, the application of the

[*]Corresponding author: Department of Civil Engineering, University of Birjand, Birjand, Iran
[†]E-mail address: m.khatibinia@birjand.ac.ir (M. Khatibinia)

methods for the damage detection is important. As a consequence, the existence of damage in structures can change their static and dynamic responses. Accordingly, various non–destructive damage identification schemes have been proposed and developed. These methods have the merit of preserving the integrity and safety of a structure. The proposed methods can be categorized into global and local strategies. Some of these methods are based on the modal responses which include natural frequencies, mode shapes and damping ratios. Many studies have revealed that mode shapes and corresponding mode shape curvatures could be considered as the best responses of structures in the damage detection procedure [9–20]. Furthermore, most of the damage detection techniques have relied on baseline information to identify the location and severity of the damage. However, some techniques don't require such information and have more flexibility in engineering applications [14]. In some studies [21, 22], two–step approaches based on the modal strain energy method and an optimization method were developed for the damage detection of structures. The application of optimization methods were also adopted and developed as effective tools in the damage detection of structures [23–31].

For many years, the wavelet transform–based methods have been successfully applied as a promising mathematical tool in order to detect the damage in structures [32–34]. In these methods, the structural responses are converted into signals. Then, the damage identification can be performed using the wavelet coefficients. Various studies have used wavelet transforms in the damage detection of two–dimensional structures such as plate structures. In the following, these studies are reviewed briefly. Fan and Qiao [35] developed a method that could identify the damage in plate structures using the Dergauss2 wavelet. By performing wavelet analysis, Douka *et al*. [36] suggested a method for the crack identification in plate structures. In this scheme, the continuous wavelet transform employed the vibration modes of plate and estimated the location and depth of cracks. A method based on the continuous wavelet transform was introduced by Rucka and Wilde [37] in order to find the location of damages in beam and plate structures. In this study, the location of the damage was revealed by the peaks of the spatial variation of the transformed responses. Huang *et al*. [38] monitored the structural degradation by using a two–dimensional continuous wavelet transform and assessing the spatially continuous variation of the structural response parameters. Xiang and Liang [39] developed a technique for detecting multiple damages in thin plates. This technique consisted of two steps: 1) identifying the damage location; 2) the estimation of the damage severity. In the work of Fan and Qiao [40], a damage identification method was developed using a damage location factor matrix and a damage severity correction factor matrix for the localization and quantification of damage in plate–type structures. The proposed method consisted of three steps: sensitive mode selection, damage localization, and damage quantification. Hajizadeh *et al*. [41] investigated the influence of the static and dynamic responses of plate structures in the damage detection process based on the 2–D discrete wavelet. The results of this study have been demonstrated using both of the static and dynamic responses in the damage detection of plate structures. The existence of noise has an important effect on the success of a process in identifying damage based on wavelet transforms. Hence, the performance of wavelet transforms for the identification of damage location under the presence of noise was discussed by some of researchers [42, 43].

The damage detection techniques were also developed based on the curvelet and

contourlet transforms. Bagheri *et al*. [44] presented a new method based on the curvelet transform for identifying the location of damage in plate structures. The results of this study demonstrated that the curvelet transform successfully detected the linear damage in plate structures. Hajizadeh *et al*. [45] also evaluated the performance of the wavelet and curvelet transforms based–damage detection of various types of damage in plate structures. The results revealed that the wavelet and curvelet transforms could accurately identify the existence, location of the damage in plate structures. Vafai and Salajegheh [46] presented the damage detection of plate structures using the contourlet transform. The results of this study demonstrated that contourlet transform could be utilized as an accessible and useful technique for the damage detection of pate structures. Jahangir *et al*. [47] used the contourlet transform for the damage localization and severity assessment of prestressed concrete slabs. Jahangir *et al*. [48] also presented the damage detection of prestressed concrete slabs using the wavelet analysis of vibration responses in the time domain. In other study implemented by Vafai and Salajegheh [49], a new damage detection based on the shearlet transform as presented for identifying the damage in plate and was compared with the wavelet, Laplacian pyramid, curvelet, and contourlet transforms.

None of the reviewed studies has been investigated the efficiency of the contourlet transform for the damage detection of plate structures in various conditions. The various conditions include single damage and multi–damages with different shapes and severities, the different supports (i.e., boundary conditions) of structures, and the higher mode shapes of structure. While, the conditions influence the ability of the contourlet transform for the damage detection of plate structures. Hence, this study presents the effect of these conditions on the performance of the contourlet transform for the damage detection of plate structures. For this purpose, the first mode shapes of a damaged plate and a reference state as intact plate are first obtained using the finite element method (FEM). In the second step, the coefficients of the contourlet transform are calculated by applying the contourlet transform to the first mode shapes. Finally, the location and approximate shape of the damage are assessed using the difference of the contourlet transform coefficients between intact and damaged structure.

2. OVERWIEW OF CONTOURLET TRANSFORM APPROACH

2.1 Laplacian pyramid

To achieve a multi–scale decomposition, the Laplacian pyramid (LP) proposed by Burt and Adelson [50] is used. The LP decomposition is shown in Fig. 1. Obviously, it is similar to that of the wavelets.

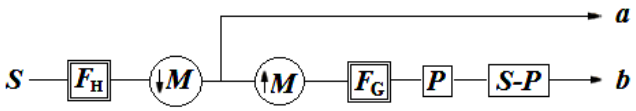

Fig. 1 Construction of Laplacian pyramid [50]

Clearly, the input image S is the firstly lowpass filtered by filter F_H. Then, it is downsampled to produce a coarse approximation a. Furthermore, it is interpolated and

passed through the synthesis filter F_G. At the next stage, the achieved image is subtracted from the original image *S*. By this way, the bandpass image *b* is obtained. This process is successively repeated on the coarser version of the image *a*. In this process, it is assumed that the LP utilizes two orthogonal filters and down sampling in each direction (i.e. *M*=diag(2,2) in Fig. 1). According to the certain regularity conditions, a unique scaling function, $\phi(t) \in L^2(R^2)$, is defined by the lowpass synthesis filter F_G. This function satisfies the following two scale equations [50, 51]:

$$\phi(t) = 2\sum_{n\in Z^2} g[n]\phi(2t-n) \tag{1}$$

and

$$\phi_{j,n} = 2^{-j}\phi(\frac{t-2^j n}{2^j}); \quad j \in Z, n \in Z^2 \tag{2}$$

in which scale, location and time are shown by indices *j*, *n* and *t*, respectively. *Z* denotes integer number. Also, $[\cdot]$ represents a matrix with discrete elements.

It should be reminded that the family $\{\phi_{j,n}\}$ forms an orthogonal basis for an approximation subspace at the scale 2^j. The LP can be considered as an oversampled filter bank. This bank includes poly phase components of the various image *b*[*n*] shown in Fig. 1 in companion with the coarse image *a*[*n*]. These components belong to different filter bank channels which have the same sampling matrix diag(2,2). The synthesis filter of the aforementioned poly phase components is denoted by F_i where $0 \le i \le 3$. These filters are the high pass ones. In an analogous manner to wavelets, a continuous function, $\psi^{(i)}(t)$, is considered for each of these filters. The functions have the subsequent shapes [51]:

$$\psi^{(i)}(t) = 2\sum_{\boldsymbol{n}\in Z^2} f_i[n]\phi(2t-n) \tag{3}$$

Inserting $\psi^{(i)}(t)$ into Eq. (3) leads to the next result:

$$\psi^{(i)}{}_{j,n}(t) = 2^{-j}\psi^{(i)}(\frac{t-2^j n}{2^j}); \quad j \in Z, n \in Z^2 \tag{4}$$

In this way, the family $\{\psi^{(i)}{}_{j,n}\}$ forms a tight frame for the subspace at the scale 2^j. It should be noted that $f_i[n]$ represents the discrete signal passed through the filter F_i.

2.2 Directional decomposition

The 2–directional filter bank (DFB) is employed for linking the edge points into linear structures, which modulate the input image and use quincunx filter banks with diamond–

shaped filters [51]. By utilizing a *l*–level tree-structured decomposition, the DFB can be efficiently implemented. In this way, 2^l sub-bands are obtained with a wedge-shaped frequency partition. Fig. 2 illustrates these sub-bands. It is seen from Fig. 2 that a bank of filters splits the 2–D frequency plane (ω) into the sub-bands. Moreover, a *l*–level DFB can generate a local directional basis for discrete signal in $L^2(Z^2)$ which is composed of the impulse responses of the 2^l directional filters and their shifts. They can be represented as [51]:

$$\left\{g_k^{(l)}[n - S_k^{(l)}m]\right\}_{0\le k<2^l, m\in Z^2} \tag{5}$$

where *m* is location and it is equal to $n\times M$.

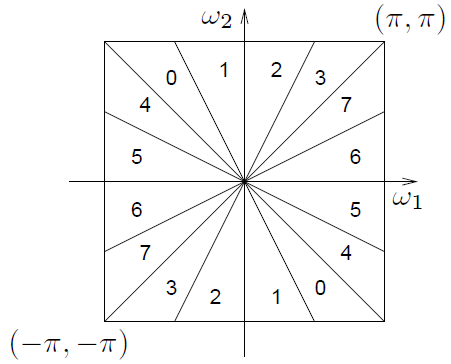

Fig. 2 Directional filter bank frequency partitioning where *l*=3 and there are 2^3=8 real wedge–shaped frequency bands [51]

The overall sampling matrices, $S_k^{(l)}$, have the following diagonal forms:

$$S_k^{(l)} = \begin{cases} \begin{bmatrix} 2^{l-1} & 0 \\ 0 & 2 \end{bmatrix} & 0 \le k < 2^{l-1} \\ \begin{bmatrix} 2 & 0 \\ 0 & 2^{l-1} \end{bmatrix} & 2^{l-1} \le k < 2^l \end{cases} \tag{6}$$

According to Do and Vetterli [51], a frame $\{\rho_{j,k,n}^{(l_j)}(x)\}$ with a redundancy ratio equal to 4/3 can span each subspace as follows:

$$\rho_{j,k,n}^{(l)}(t) = \sum_{m\in Z^2} g_k^{(l)}[m - S_k^{(l)}n]\psi^{(i)}{}_{j,n}(t); \quad j \in Z, n \in Z^2 \tag{7}$$

Hence, the coefficients of the contourlet transform can be achieved by applying the equations introduced in the next Section.

2.3 Contourlet transform

Do and Vetterli [51] proposed the contourlet transform as a two–dimensional (2–D) image representation method. This transform has been constructed based on non–separable filter banks and provided an efficient directional multi–resolution image representation. The contourlet transform approach utilizes a double filter bank technique in the discrete domain. The structure of the contourlet transform is depicted in Fig. 3.

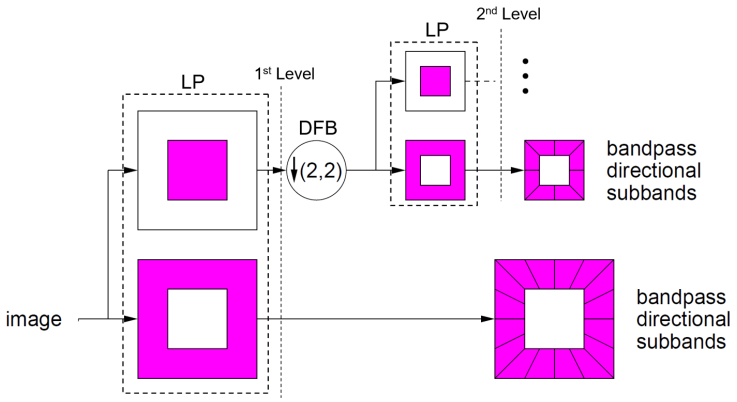

Fig. 3 A flow graph of the contourlet transform [34]

The image is first decomposed into sub bands by the Laplacian pyramid and then each detailed image is analyzed by the directional filter banks. As can be seen from Fig. 3, the transform includes two steps. Firstly, the sub-band decomposition is carried out; and at the second stage, the directional transform is implemented [51]. At first stage of the contourlet transform, the LP approach is used for capturing point discontinuities. Then, the DFB approach is implemented to link them in order to constructing linear structures. The contourlet transform has the merits of multi-resolution, localization, directionality, critical sampling and anisotropy. As a result, this transform can efficiently represent edges and other singularities along curves, in contrast to wavelet transform. In Fig. 4, the frequency partition of the contourlet transform is presented. According to Fig. 4, the 8-direction decomposition is used in the finest scale. Moreover, sub-bands 1–4 correspond to the most horizontal directions, while sub-bands 5–8 correspond to the most vertical ones.

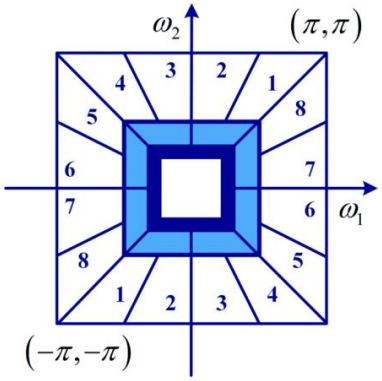

Fig. 4 Frequency partition of the contourlet transform [51]

It is assumed that an input image $f(x,y)$ is decomposed into bandpass images by using the contourlet transform of J level LP and l_j directions at each scale. Thus, the whole decomposition can be represented as follows [51]:

$$f(x,y) \to \{a_J, b_1^{(l)}, b_2^{(l)}, \ldots, b_{J-1}^{(l)}, b_J^{(l)}\} \tag{8}$$

$$b_j^{(l)} = \{d_{j,1}^{(l)}, d_{j,2}^{(l)}, \ldots, d_{j,2^{l_j}}^{(l)}\} \tag{9}$$

where a_J and $d_{j,k}^{(l)}$ are approximate and detail coefficients, respectively, and are given by:

$$a_J[n] = \left\langle f, \phi_{J,\boldsymbol{n}} \right\rangle \tag{10}$$

$$d_{j,k}^{(l)}[n] = \left\langle f, \rho_{j,k,\boldsymbol{n}}^{(l)} \right\rangle \tag{11}$$

where $\langle\ \rangle$ is an inner product.

3. FINITE ELEMENT MODEL OF DAMAGE DETECTION

By monitoring the structural dynamic responses such as mode shapes, the existence of damage can be identified in plate structures. As previously mentioned, the mode shapes of damaged and intact plates are required in the damage detection procedure. To achieve this purpose, the free vibration analysis of plate structure is carried out using the finite element method (FEM). This work deals with the damage detection of rectangular plates. After the occurrence of damage, it is assumed that the plate is cracked. In Fig. 5, a rectangular plate with one damage (or crack) is schematically depicted. The thickness, length and width of the plate are shown by t, L and B, respectively. Furthermore, it is assumed that the damage occurred in the plate is a linear damage. Its length and width are W and D. Its location is specified by L_1 and B_1. Also, α is the angle of the crack with the horizontal edge.
In this study, the damage is modeled as a reduction in Young's modulus of elements. Young's modulus of a damaged element is defined as:

$$E_d = E(1-d) \tag{12}$$

where E_d and E are the Young's modulus of the damaged and undamaged elements, respectively; and d indicates the damage severity. This method of modeling damage was utilized for plate structures by other researchers [7, 44–46].

Based on the Hamilton principle [52], the equation of dynamic equilibrium for the Mindlin plate is expressed as:

$$\boldsymbol{M}\,\ddot{\boldsymbol{u}}(t) + \boldsymbol{K}\,\boldsymbol{u}(t) = \boldsymbol{f}(t) \tag{13}$$

in which $\boldsymbol{f}$, $\boldsymbol{M}$ and $\boldsymbol{K}$ are the force vector and mass and stiffness matrices, respectively. Furthermore, $\ddot{\boldsymbol{u}}$ and $\boldsymbol{u}$ are the acceleration and displacement functions, respectively.

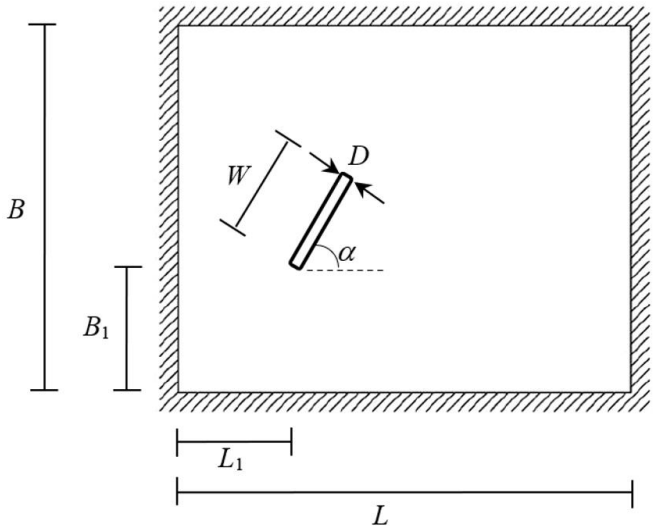

Fig. 5 Geometry of a plate structure with linear damage

If a harmonic motion is assumed, the natural frequencies and modes of plate vibration can be obtained in the framework of Eigen–problem. This problem is defined as follows:

$$(\boldsymbol{K} - \omega_i^2 \boldsymbol{M})\boldsymbol{\varphi}_i = \boldsymbol{0}\ , \quad i = 1, 2, \ldots, n_m \tag{14}$$

where ω_i is the natural frequency of the ith mode; and $\boldsymbol{\varphi}_i$ is the ith mode shape vector of vibration. n_m is the number of structural modes. In this study, the first mode shape (i.e. $\boldsymbol{\varphi}_1$) is utilized in the damage detection process.

4. CONTOURLET TRANSFORM FOR DAMAGE DETECTION

In this study, the contourlet transform using the first mode shape of plate structures is presented for identifying the existence of the damage which produces small discontinuities in the structural responses at the damaged locations. These discontinuities cannot be observed by comparing the responses of damaged plate with those of intact plates. It is worth pointing out that the contourlet coefficients can detect the discontinuities, which are obtained based on the difference of the first mode shape between the intact and damaged plate structures. The following steps of the proposed method are implemented in order to detect the damage in a rectangular plate:

1. At the first stage, the first mode shapes of a damaged and intact plate structure are determined by performing the modal analysis. To achieve this purpose, the finite element analysis of intact and damaged plate structure is coded in MATLAB software [53].

2. The contourlet transform is applied to the first mode shapes of the intact and damaged plate structures which are considered as an image. In this step, first, each mode shape is decomposed into sub–bands by LP transform, and details are obtained. Afterward, the details of each mode shape are analyzed by DFB. Eventually, the coefficients of the contourlet transform expressed in Eqs. (10) and (11) are chosen for the mode shapes.
3. The damage index is calculated based on the difference of the coefficients for each element node of damaged and intact plates. The damage index of the *i*th node, DI_i, is defined as follows [45]:

$$DIi = C_i^d - C_i^u \tag{15}$$

where C_i^d and C_i^u are the approximate or detail coefficients of the contourlet transform for *i*th node in damaged and intact plates. The coefficients are calculated based on Eqs. (10) and (11).

4. In the final step, the damage is detected by plotting the damage index in all of the nodes of plate elements.

It is noted that the coefficients of the first level of the contourlet transform are used in this study. Hence, the dimensions of studied plate structures are half in the damage detection procedure. The issue (so-called as the decomposition procedure of each level) were completely expressed in Hajizadeh *et al*. [45]

5. NUMERICAL SIMULATIONS

In this section, the performance of the contourlet transform is assessed for the damage detection for plate structures with several examples and the effective conditions.

5.1 Case1: a linear damage

A rectangular plate with the length $L = 250\,\text{cm}$, the width $B = 250\,\text{cm}$ and the thickness $t = 5\,\text{cm}$ is considered as the first example. The material properties of the plate include Young's modulus of $E = 2.1\times10^6\,\text{kg/cm}^2$, mass density of $\rho = 0.00785\,\text{kg/cm}^3$, and Poisson's ratio of $v = 0.33$. In this example, it is assumed that a linear damage with the length of $W = 20\,\text{cm}$, the width of $D = 3\,\text{cm}$, $\alpha_1 = 90^\circ$ is occurred in the plate and the location coordinates of the damage are $L_1 = 105\,\text{cm}$ and $B_1 = 125\,\text{cm}$. The damage severity, *d*, is also equal to10%. A comparison between the first mode shapes of damaged and intact plate is depicted in Fig. 6.

Since no difference is observed between the first mode shape of the damaged plate and the intact plate, it is quite difficult to reveal the difference. Hence, the contourlet transform is applied to the first mode shape of the intact and damaged plate structures and the damage index defined in Eq. (22) are calculated. The plot of the damage index is shown in Figs. 7 and 8. As revealed from Figs. 7 and 8, the peak values of the damage index are obviously created at the position of the damage. Hence, the contourlet transform can detect the location of damage. It is noted that the approximation coefficients and detail coefficients of the contourlet transform are calculated based on Eqs. (10) and (11), respectively.

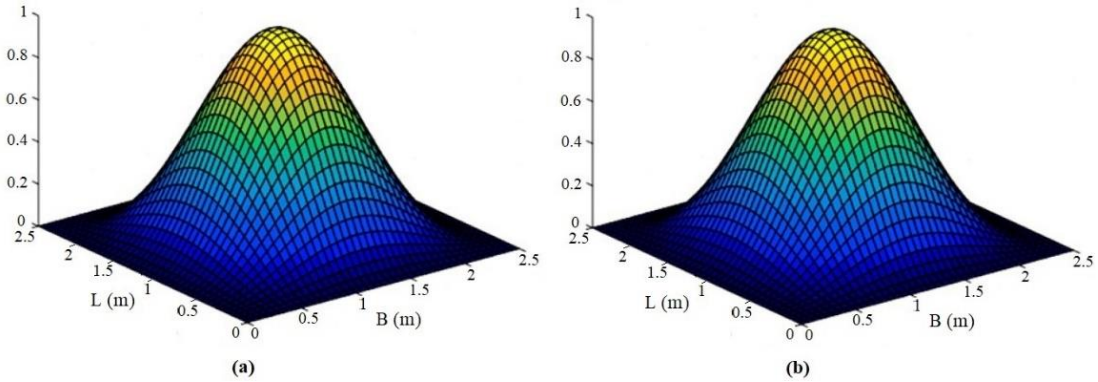

Fig. 6 First mode shape for the plate: (a) without damage (b) with damage

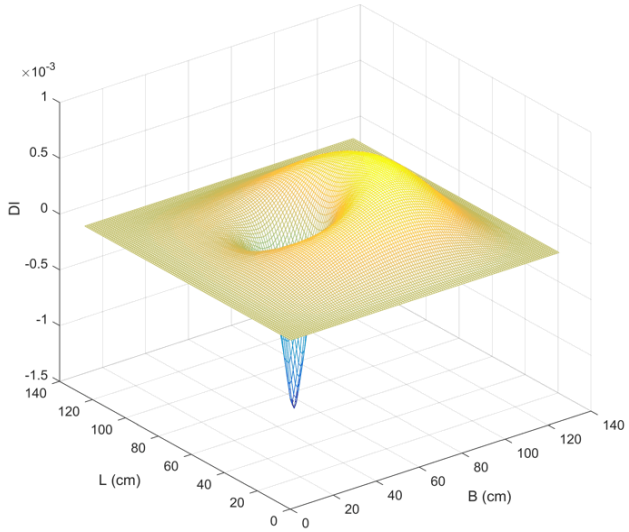

Fig. 7 Damage index based on the approximation coefficients of the contourlet transform

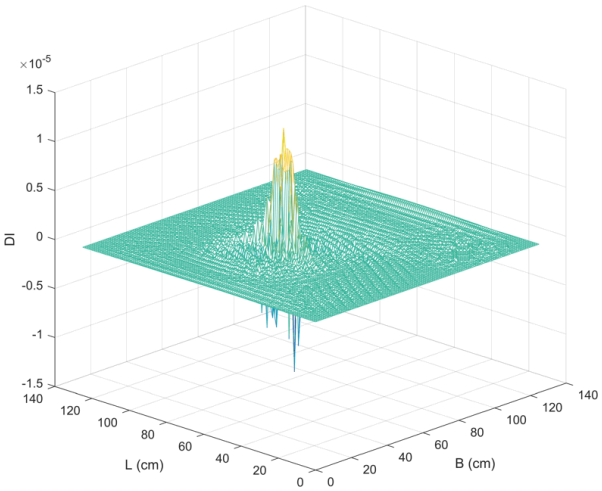

Fig. 8 Damage index based on the detail coefficients of the contourlet transform

Fig. 9 also shows the values of the damage index which are obtained based on the 2-D vertically added detail coefficients of the contourlet transform. It can be seen from Fig. 9 that the contourlet transform can identify the location of the damage. It is noted that this example was considered by Hajizadeh *et al*. [45] and the damage detection process was implemented using the 2-D discrete wavelet transform. For the comparison of the contourlet transform with the 2-D discrete wavelet transform, the damage quantification results obtained based on the 2-D discrete wavelet transform are depicted in Fig. 10. This figure is related to the damage index determined from the 3-D of the detail coefficients of the wavelet transform. By the comparison of the results shown in Figs. 8 and 10, it is revealed that the performance of the contourlet transform is similar to that of the 2-D discrete wavelet transform.

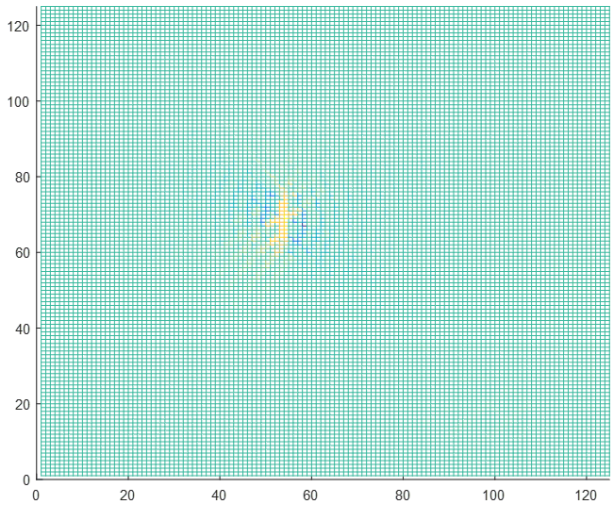

Fig. 9 Damage index based on the 2–D detail coefficients of the contourlet transform

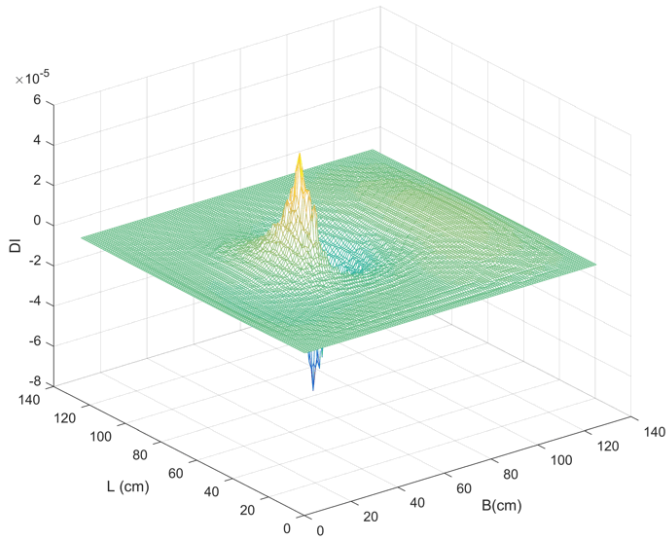

Fig. 10 Damage index for the detail coefficients of the wavelet transform [45]

5.2 Case 2: an oblique linear damage

In this example, a fixed–supported rectangular plate with the length $L = 600$ cm, the width $B = 600$ cm, and the thickness $t = 2$ cm is presented. Bagheri *et al*. [44] investigated the damage detection of this plate using the curvelet transform. The material properties of the plate include Young's modulus of $E = 2.1\times10^{6}$ kg/cm^2, mass density of $\rho = 0.0025$ kg/cm^3 and Poisson's ratio of $v = 0.2$. It is assumed that the damage of plate induced in the plate structure with the length of $W = 19$ cm, the width of $D = 1$ cm and $\alpha = 45^{\circ}$ and the started location coordinates of the damage are $L_1 = 406$ cm and $B_1 = 445$ cm. The damage was represented using the elements with reduced thickness. Hence, the damage severity, *d*, is assumed to be 20%. In order to identify the damage in this plate, the contourlet transform is applied to the difference between the intact and damaged plate structures. The results of the damage detection are depicted in Figs. 11 and 12 by determining the details and approximation coefficients of the contourlet transform. Results are related to the damage index of the detail and approximation coefficients of the contourlet transform.

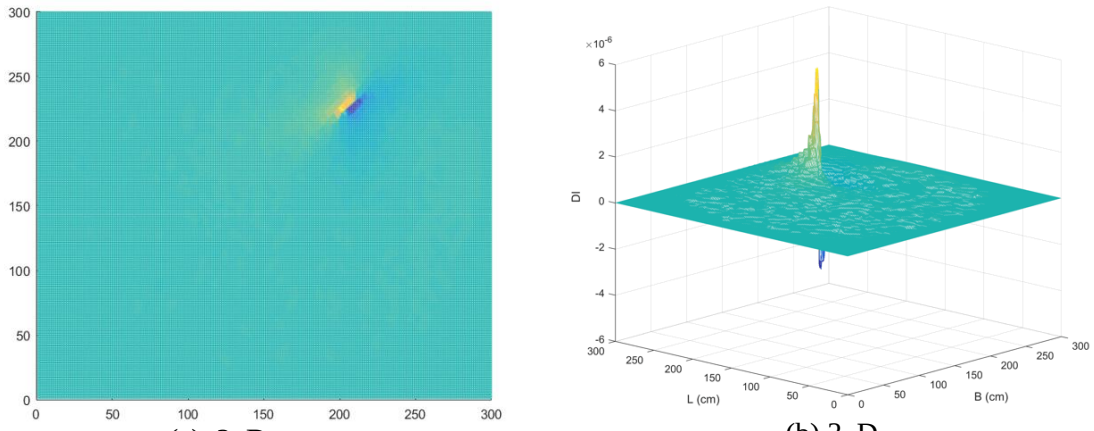

(a) 2–D (b) 3–D

Fig. 11 Damage index for the 2–D and 3–D detail coefficients of the contourlet transform

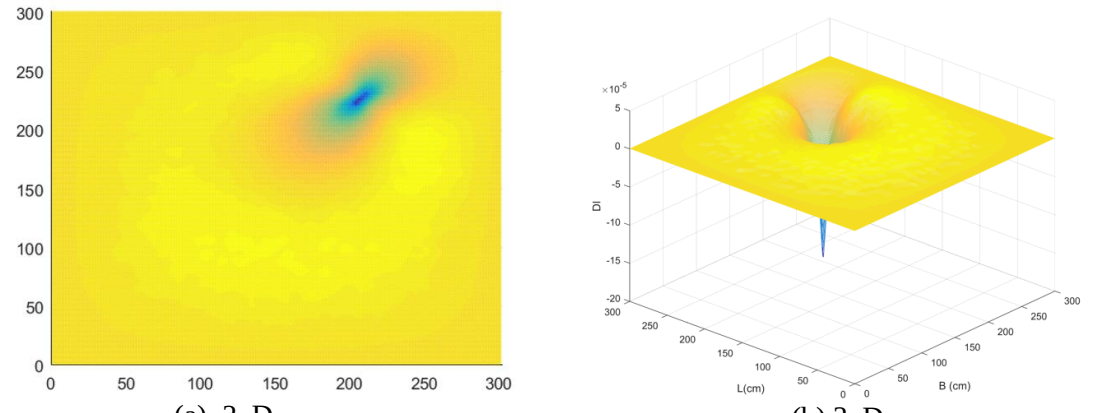

(a) 2–D (b) 3–D

Fig. 12 Damage index for the 2–D and 3–D approximation coefficients of the contourlet transform

It can be seen from Figs. 11 and 12 that this linear damage in the plate structure is detected and localized using the contourlet transform. Based on Figs. 11 and 12, it can be concluded that the contourlet transform can identify the approximate shape of the damage. Furthermore, as observed from Figs. 11 and 12, the peak values of the damage index are occurred at the location of the damage. Based on the comparison of this study with that presented by Bagheri *et al*. [44], it can be concluded that the results of the contourlet transform are similar to those of the curvelet transform. The results also demonstrate that the contourlet transform can identify the approximate shape of the damage.

5.3 Case 3: a curved damage

For the third case, a fixed–supported rectangular plate with dimensions $L = 500\,\text{cm}$, $B = 500\,\text{cm}$, $t = 1\,\text{cm}$ is considered and shown in Fig. 13. The material properties of the plate are assumed to be Young's modulus of $E = 2.1\times10^{6}\,\text{kg/cm}^2$, mass density of $\rho = 0.00785\,\text{kg/cm}^3$ and Poisson's ratio of $v = 0.3$. In this example, a curved damage with the with a radius of $R = 70\,\text{cm}$ is a part of a circle and the started location coordinates of the damage are $L_1 = 214.7\,\text{cm}$ and $B_1 = 250\,\text{cm}$. The different severities of damage including 10%, 5% and 2% are considered as the reduce of Young's modulus in order to investigate the effectiveness of the contourlet transform for different severities of damage.

The results for the different severities of the damage in the plate are shown in Figs. 14 to 16. As it can be seen from Figs. 14 to 16, the contour transform can identify the damage which has the severity higher than 5%. The results also demonstrate the efficiency and applicability of the contour transform in the detection of the location and approximate shape of the damage. Therefore, the severity of the damage influences the performance of the contour transform.

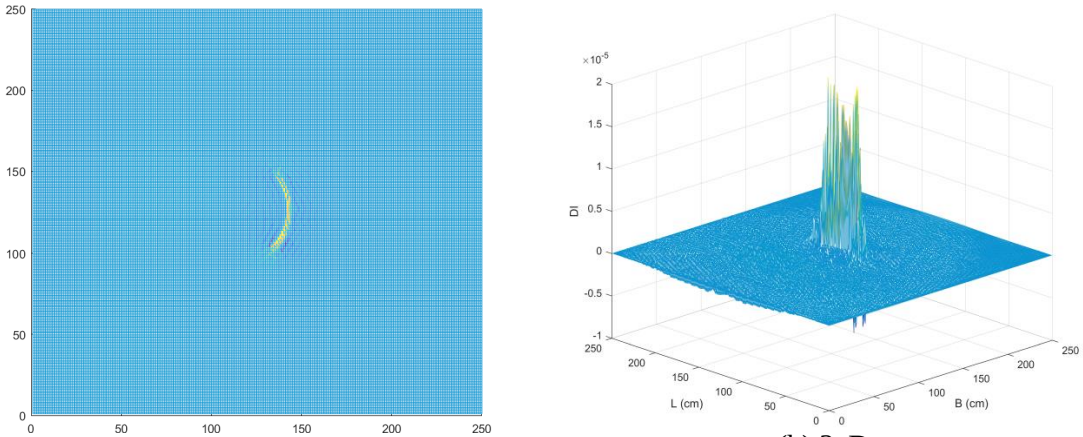

(a) 2–D (b) 3–D

Fig. 14 The damage index for 10 percent damage

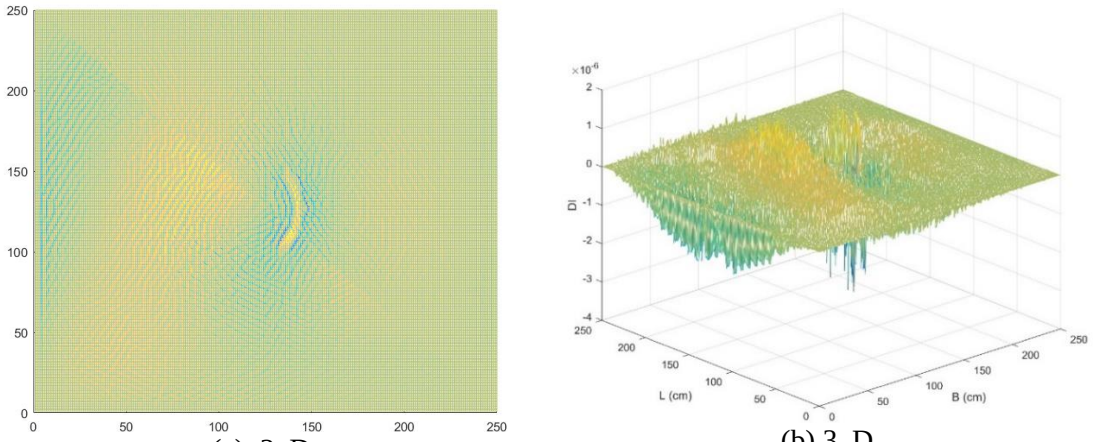

(a) 2–D (b) 3–D

Fig. 15 The damage index for 5 percent damage

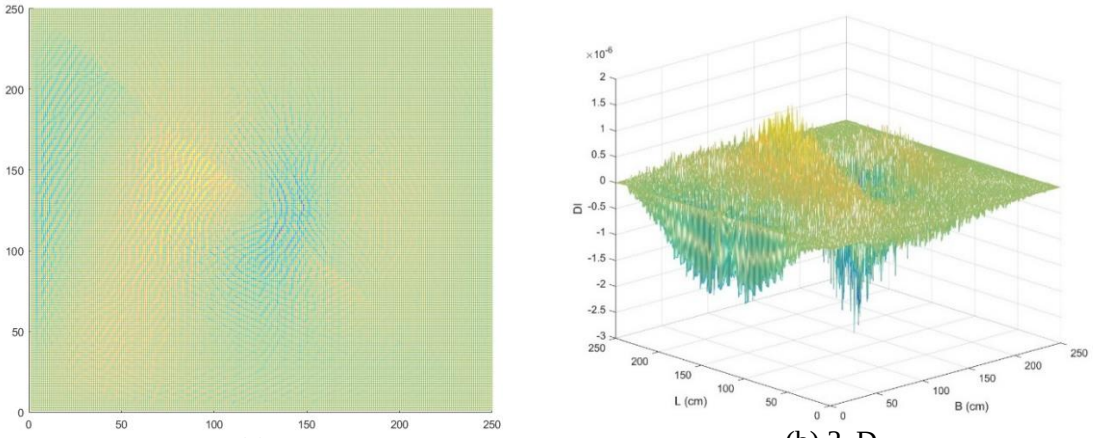

(a) 2–D (b) 3–D

Fig. 16 The damage index for 2 percent damage

5.4. Case 4: three damages

The rectangular plate with the properties described in section 5.3 is considered in this example. In order to investigate the capability of the contour transform in the detection process of plate structures with multi damages, it is assumed that three damages are occurred in the plate and shown in Fig. 17. The damages consist of a liner damage with the length of $W = 30\,\text{cm}$, the width of $D = 3\,\text{cm}$, a square damage with the length of $W = 15\,\text{cm}$, the width of $D = 15\,\text{cm}$ and a curved damage with a radius of $R = 40\,\text{cm}$, the width of $D = 3\,\text{cm}$. The location coordinates of the liner, square and curved damages are $L_1 = 80\,\text{cm}$ and $B_1 = 80\,\text{cm}$, $L_2 = 115\,\text{cm}$ and $B_2 = 115\,\text{cm}$, and $L_3 = 205.8\,\text{cm}$ and $B_3 = 73.3\,\text{cm}$, respectively.

In the first scenario, the severity of all damages is assumed to be 20%. The results of the damage detection using are shown in Fig. 18. As seen from Fig. 18, the peak values of the damage index obtained based on the detail coefficients are created in the location of the damages. Thus, it can be concluded that the contourlet transform efficiently identifies the location of multi–damages with the equal severity induced in the plate structures.

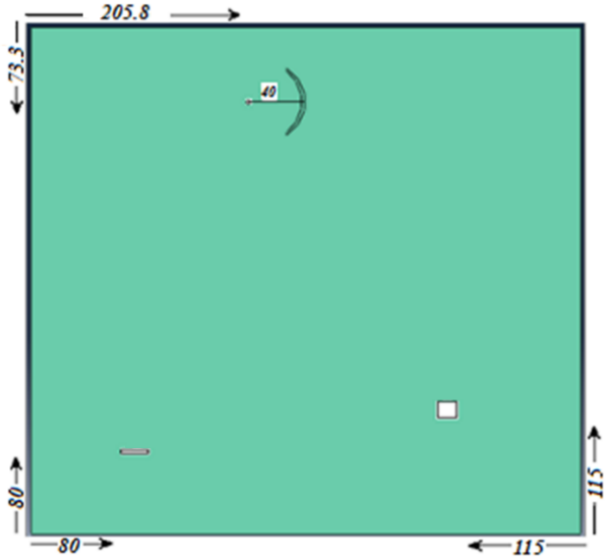

Fig. 17 Geometry of the plate structure with the three damage (unit: cm)

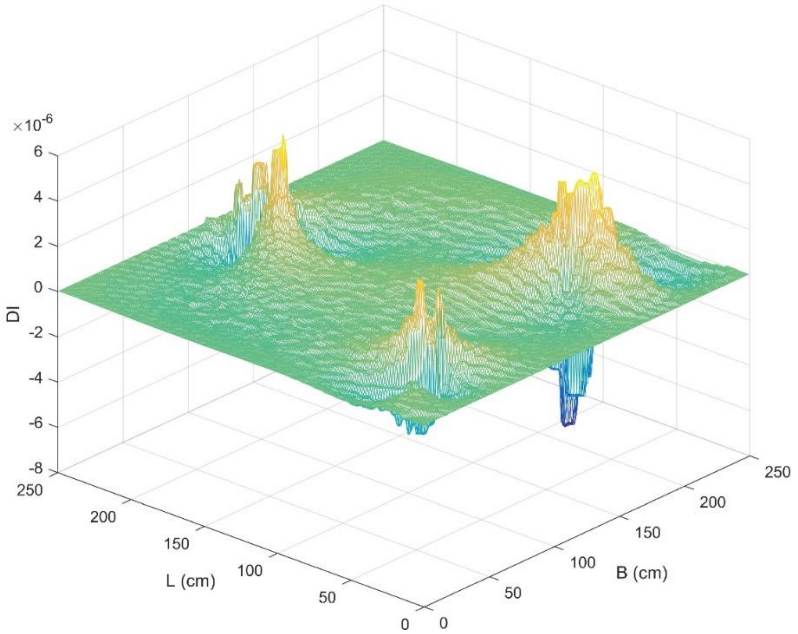

Fig. 18 The damage index for the detail coefficients of the contourlet transform

In the second scenario, the severity of the liner, square and curved damages are assumed to be equal 7%, 13% and 20%, respectively. The results of the damage identification are depicted in Fig. 19. It can be observed from Fig. 19 that the peak values of the damage index for the detailed coefficients are created in the location of the damages. However, the high damage indices corresponding to the damages with high severity influence the detection of the damage with low severity. Hence, the damage with low severity may not be identified clearly.

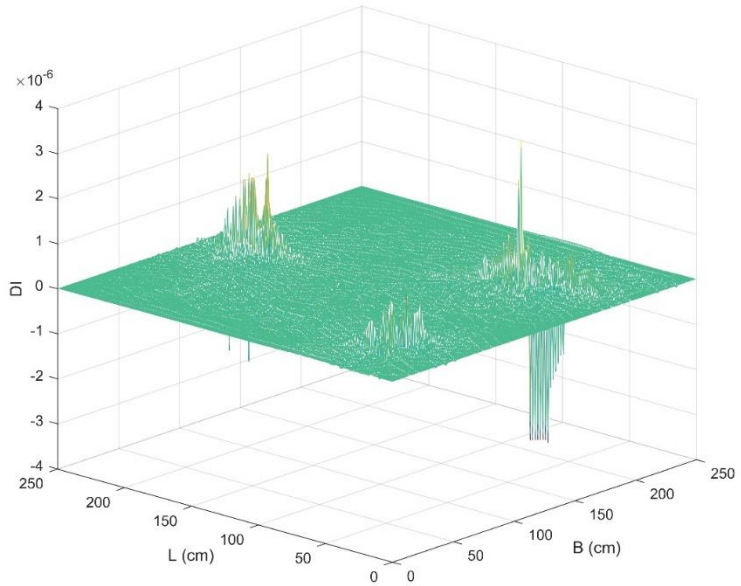

Fig. 19 The damage index for the detail coefficients of the contourlet transform

5.5. Case 5: different boundary conditions

In order to assess the effect of boundary conditions, a rectangular plate with the length $L = 400$ cm, the width $B = 400$ cm and the thickness $t = 5$ cm is selected in this example and is shown in Fig. It is assumed that a damage with 30×30 cm is occurred in the distance of 70 cm from the left corner of the plate as shown in Fig. 20. The damage severity is also assumed to be 15% reduction in elasticity modulus. For the effect of boundary conditions in the damage detection of plate structures, the different boundary conditions are selected in modeling the finite element of the plate.

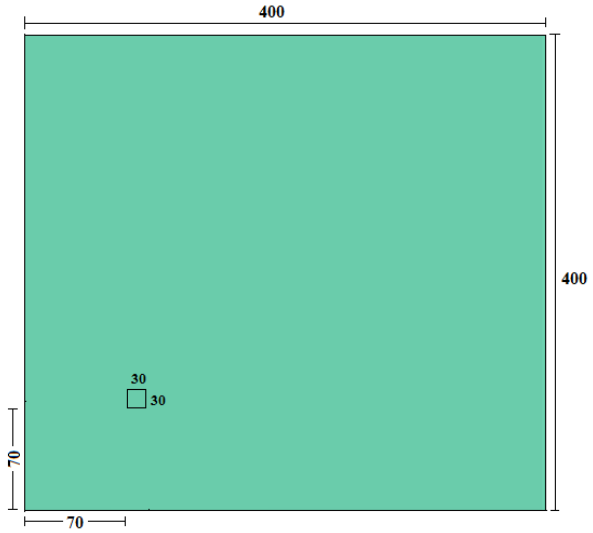

Fig. 20 Geometry of the plate structure with an area of 30×30 cm as damage (unit: cm)

For this purpose, four cases of the boundary conditions are selected for the damage detection of the rectangular plate and consist of: 1) four fixed supports, 2) four pin supports, 3) a fixed support in the left edge of plate, 4) a support in the right edge of plate. It is noted that in the three and four cases other edges of the plate are free. Figs. 21 to 23 show the obtained results of the contourlet transform for the damage assessment of the cases (2) to (4) in the plate. For the case (1), the numerical results are reported in Fig. 11. It is observed that the contour transform can accurately find the location of the damage in the cases (1) and (2). In the case (3), the location of the damage with satisfactory precision is identified, but the contourlet transform cannot reveal the actual damage in the case (4)

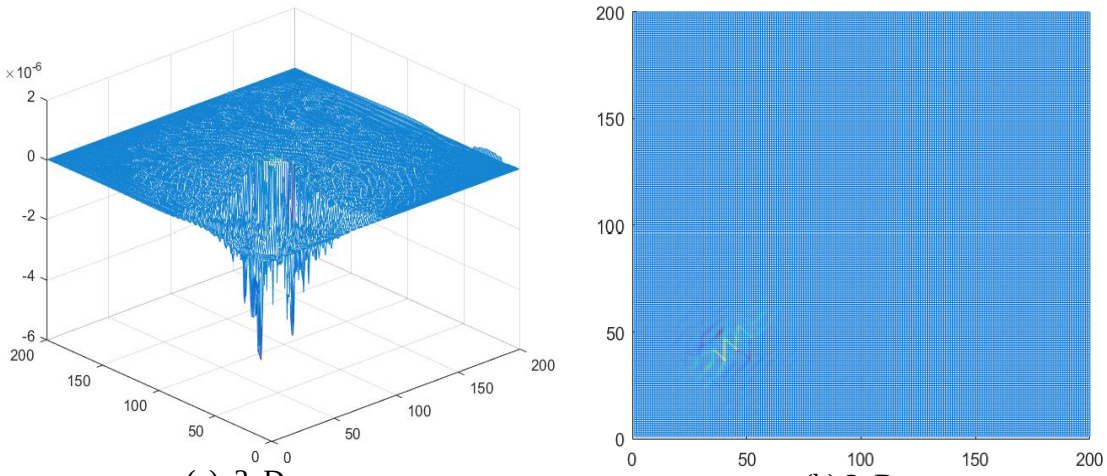

(a) 3–D (b) 2–D

Fig. 21 The results of the damage detection for case (2)

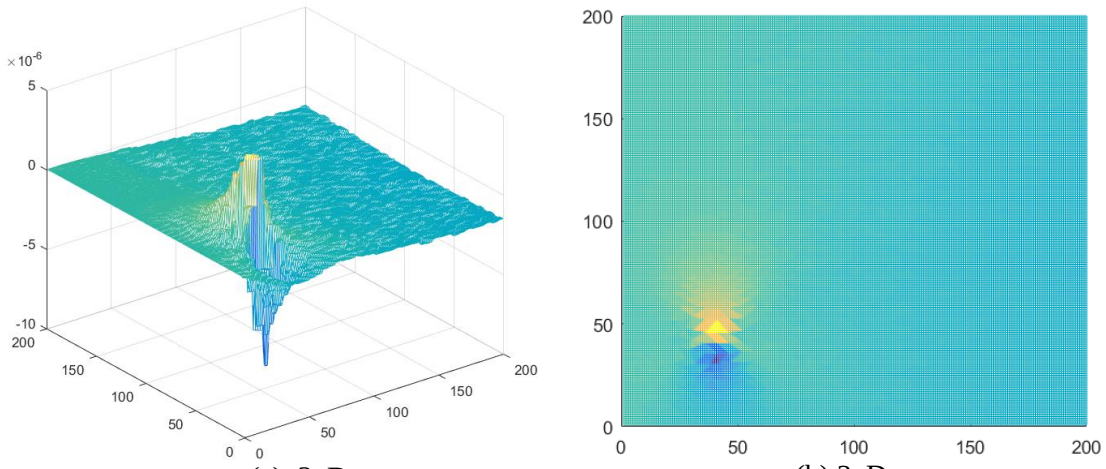

(a) 3–D (b) 2–D

Fig. 22 The results of the damage detection for case (3)

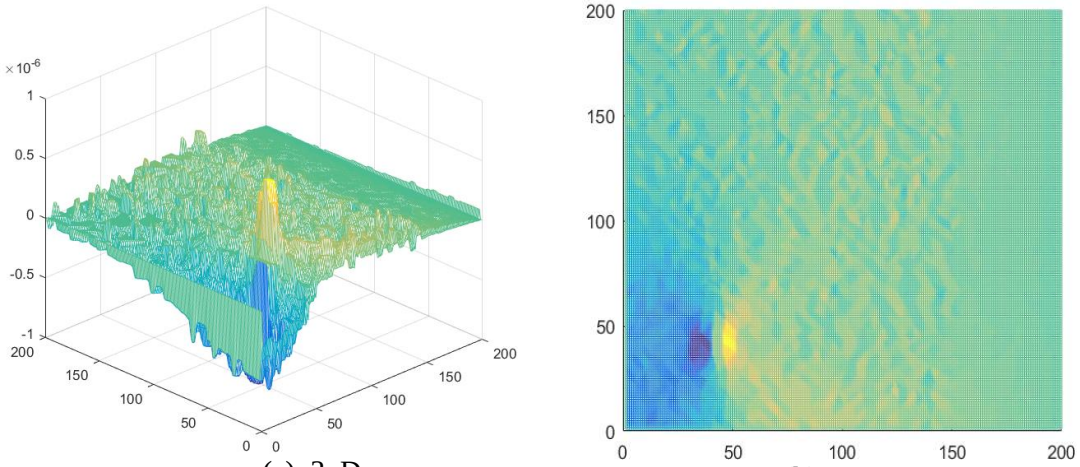

(a) 3–D (b) 2–D

Fig. 23 The results of the damage detection for case (4)

5.6. Case 6: effect of higher–order mode shapes

In this example, the effectiveness and performance of the contourlet transform are also investigated by using the higher–order mode shapes. For this purpose, the plate with an oblique linear damage presented in section 5.2 is considered. The results of the damage detection for the second to fifth mode shapes are shown in Fig. 24.

It is seen from Fig. 24 that the location of the damage cannot be identified by using the higher mode shapes. In fact, since the peak of the detail coefficients of the contourlet transform is occurred at the change of the curvature location, the location of damage cannot be detected by the contourlet transform. In other words, the change in the curvature of the higher mode shapes causes a jump in the contourlet transform coefficient and the contradiction in the detection of the damage.

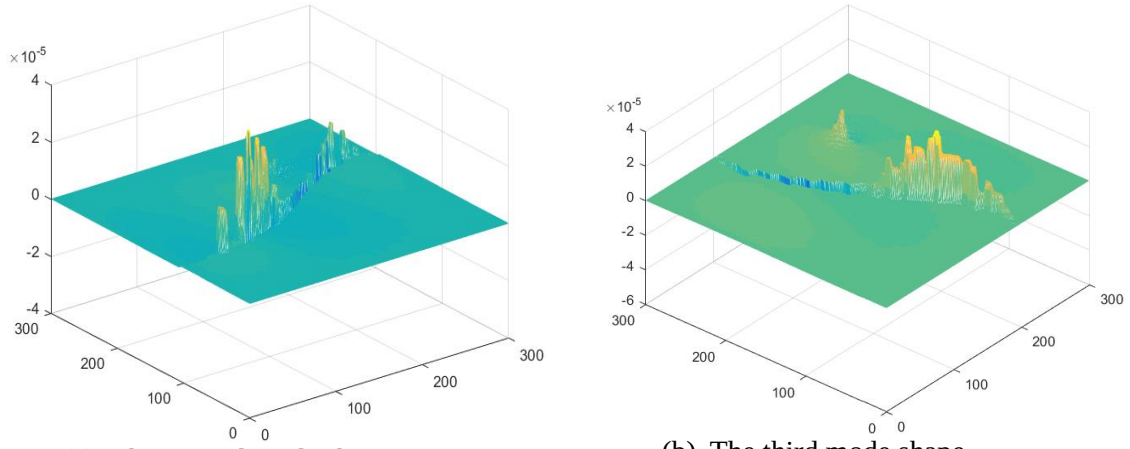

(a) The second mode shape (b) The third mode shape

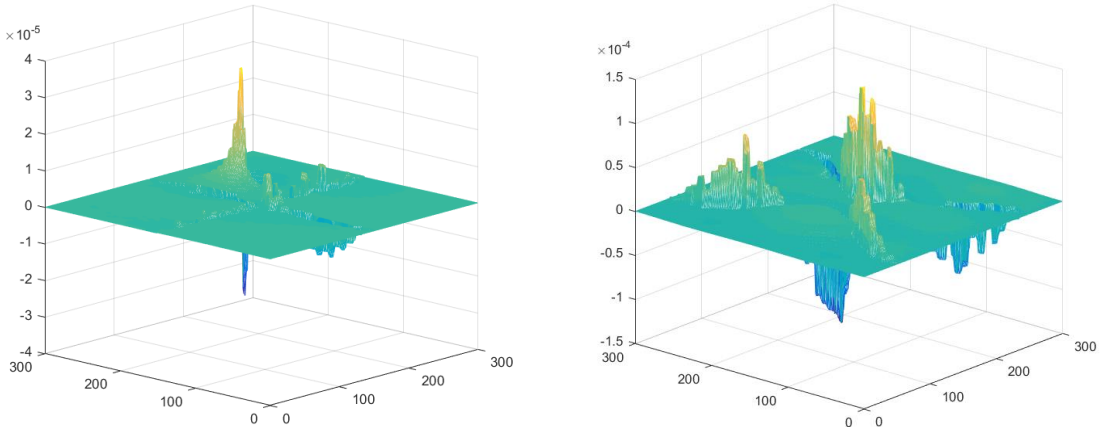

(c) The fourth mode shape (d) The fifth mode shape

Fig. 24 The damage index based on the detail coefficients of the contourlet transform for the second to fifth mode shapes

6. CONCLUSIONS

In this study, the assessment of the contourlet transform with the effective conditions was investigated in order to identify the location of damages in plate structures using the first mode shapes corresponding to the damaged and intact structures. To achieve this purpose, the contourlet transform was used to identify the difference between the obtained mode shapes of a damaged plate and a reference state as the intact plate. The damage detection process was also implemented without regard to noise. The observation of the results indicates that the contourlet transform can detect the existence, location and approximate shape of one or multi-damages in plate structures. Furthermore, the following results can be drawn from this study:

- Due to the displacements of a plate structure in the first mode shape, the single damage with different shapes can be detected by the contourlet transform.
- In plate structures with single damage and multi–damages, the location of the damage with the severity more than 5% can be identified very well.
- If the difference of the percentage severities in plate structure with multi–damages is high, the damage detection with the smaller percentage severity is influenced by the damages with the larger percentage severity, and its location cannot be identified.
- The numerical results reveal that the boundary conditions are the important factors in the damage identification using the contourlet transform.
- Due to the displacements of a plate structure in the first mode shape, this mode shape can be considered as the best response of plate structure in the damage detection procedure.
- The change in the curvature of the higher mode shapes causes a jump in the contourlet transform coefficient and the contradiction in the detection of the damage. Hence, the higher mode shapes can’t be used in the damage detection using the contourlet transform.

REFERENCES

1. Naseralavi SS, Salajegheh J, Fadaee MJ. Detection of damage in cyclic structures using an eigenpair sensitivity matrix, *Comput Struct* 2012; **110**: 43–59.
2. He YW, Zhu S. Progressive damage detection based on multi–scale wavelet finite element model: numerical study, *Comput Struct* 2013; **125**: 177–86.
3. Naseralavi SS, Salajegheh E, Fadaee MJ, Salajegheh J. A novel sensitivity–based method for damage detection of structures under unknown periodic excitations, *J Sound Vib* 2014; **333**: 2776–803.
4. Ghiasi R, Ghasemi MR. Optimization–based method for structural damage detection with consideration of uncertainties: a comparative study, *Smart Struct Syst* 2018; **22**(5): 561–74.
5. Arefi Sh, Gholizad A, Seyedpoor SM. A modified index for damage detection of structures using improved reduction system method, *Smart Struct Syst* 2020; **25**(1): 1–22.
6. Mohammadizadeh MR, Jahanfekr E, Shojaee S. Damage detection in thin plates using a gradient–based second–order numerical optimization technique, *Int J Optim Civil Eng* 2020; **4**(10): 571–94.
7. Hajizadeh AR, Khatibinia, Fundamental mode shape–based damage detection in arbitrary shaped plates using a hybrid of contourlet transform and Delaunay triangulation, *Structures* 2023; **58**: 105631.
8. Mahdavi VR, Kaveh A. Structural damage identification based on change in neutral frequencies using three multi–objective metaheuristic algorithms, *Int J Optim Civil Eng* 2024; **14**(3): 337–54.
9. Kaveh A, Javadi SM, Maniat M. Damage assessment via modal data with a mixed particle swarm strategy, ray optimizer, and harmony search, *Asian J Civ Eng* 2014, **15**(1): 95–106.
10. Kaveh A, Maniat M. Damage detection in skeletal structures based on charged system search optimization using incomplete modal data, *Int J Civ Eng* 2014, **12**(2): 291–98.
11. Hamad WI, Owen JS, Hussein MFM. Modeling the degradation of vibration characteristics of reinforced concrete beams due to flexural damage, *Struct Control Health* 2015; **22**(6): 939–67.
12. Hsu TY, Liao WI, Shiao SY. A pseudo local flexibility method for damage detection in hyperstatic beams, *Struct Control Health* 2015; **22**(4): 682–93.
13. Kaveh A, Zolghadr A. An improved CSS for damage detection of truss structures using changes in natural frequencies, *Adv Eng Softw* 2015, **80**: 93–100.
14. Alves V, Cury A, Roitman N, Magluta C, Cremona C. Novelty detection for SHM using raw acceleration measurements, *Struct Control Health* 2015; **22**(9): 1193–1207.
15. Kaveh A, Maniat M Damage detection based on MCSS and PSO using modal data, *Smart Struct Syst* 2015; **15**(5), 1253–70.
16. Dworakowski Z, Kohut P, Gallina A, Holak K, Uhl T. Vision–based algorithms for damage detection and localization in structural health monitoring, *Struct Control Health* 2016; **23**(1): 35–50.

17. Kaveh A, Hoseini Vaez SR, Hosseini P, Fallah N. Detection of damage in truss structures using Simplified Dolphin Echolocation algorithm based on modal data, *Smart Struct Syst* 2016, **5**(18): 983–1004.
18. Ooijevaar TH, Warnet LL, Loendersloot R, Akkerman R, Tinga T. Impact damage identification in composite skin–stiffener structures based on modal curvatures, *Struct Control Health* 2016; **23**(2): 198–217.
19. Kaveh A, Rahmani P, Dadras A. Guided water strider algorithm for structural damage detection using incomplete modal data, *J Sci Technol Trans Civ Eng* 2021; **46**: 771–88.
20. Rucevskis S, Janeliukstis R, Akishin P, Chate A. Mode shape–based damage detection in plate structure without baseline data, *Struct Control Health* 2016, **23**: 1180–93.
21. Kaveh A, Zolghadr A. Cyclical parthenogenesis algorithm for guided modal strain energy based structural damage detection; *Appl Soft Comput* 2017, **57**: 250–64.
22. Kaveh A, Zolghadr A. A guided modal strain energy based approach for structural damage identification using Tug of War Optimization algorithm, *J Comput Civ Eng ASCE* 2017, **31**(4): 04017016.
23. Kaveh A, Zolghadr A, An improved charged system search for structural damage identification in beams and frames using changes in natural frequencies, *Int J Civ Eng* 2012; **2**(3): 321–40.
24. Kaveh A, Mahdavi VR. Damage identification of truss structures using CBO and ECBO algorithms, *Asian J Civ Eng* 2016, **1**(17): 75–89.
25. Kaveh A. *Applications of Metaheuristic Optimization Algorithms in Civil Engineering*, Springer, Switzerland, 2017.
26. Kaveh A, Dadras A. Structural damage identification using enhanced thermal exchange optimization algorithm, *Eng Optimiz* 2018, **50**(3): 430–451.
27. Kaveh A, Rahmani P, Dadras EA. A multi-stage damage detection approach using graph theory and water strider algorithm, *J Sci Technol Trans Civ Eng* 2021, **46**: 33–54
28. Kaveh A, Hoseini Vaez SR, Hosseini P. Enhanced vibrating particle system algorithm for damage identification of truss structure, *Sci Iran* 2019, **1**(26): 246–56.
29. Kaveh A, Hoseini Vaez SR, Hosseini P. A new two-phase method for damage detection in skeletal structures, *J Sci Technol Trans Civ Eng* 2019, **43**: 49–65.
30. Kaveh A, Hosseini SM, Zaerreza A. Boundary strategy for optimization–based structural damage detection problem using metaheuristic algorithms, *Period Polytech Civ Eng* 2021, 65(1): 150–67.
31. Kaveh A, Hosseini SM, Akbari H. Efficiency of plasma generation optimization for structural damage identification of skeletal structures based on a hybrid cost function, *J Sci Technol Trans Civ Eng* 2021, **45**: 2069–90.
32. Nagarajaiah S, Basu B. Output only modal identification and structural damage detection using time frequency & wavelet techniques, *Earthq Eng Eng Vib* 2009; **8**(4): 583–605.
33. Basu B, Nagarajaiah S, Chakraborty A. Online identification of linear time–varying stiffness of structural systems by wavelet analysis, *Struct Health Monit* 2008; **7**(1): 21–36.
34. Cao MS, Qiao PZ. Integrated wavelet transform and its application to vibration mode shapes for damage detection of beam–type structures, *Smart Mater Struct* 2008; **17**(5): 055014.

35. Fan W, Qiao P. A 2–D continuous wavelet transform of mode shape data for damage detection of plate structures, *Int J Solids Struct* 2009; **46**: 4379–95.
36. Douka E, Loutridis S, Trochidis A. Crack identification in plates using wavelet analysis, *J Sound Vib* 2004; **270**: 279–95.
37. Rucka M, Wilde K. Application of continuous wavelet transform in vibration based damage detection method for beams and plates, *J Sound Vib* 2006; **297**: 536–50.
38. Huang Y, Meyer D, Nemat–Nasser S. Damage detection with spatially distributed 2D continuous wavelet transform, *Mech Mater* 2009; **41**: 1096–107.
39. Xiang J, Liang M. A two–step approach to multi–damage detection for plate structures, *Eng Fract Mech* 2012; **91**: 73–86.
40. Fan W, Qiao PZ. A strain energy–based damage severity correction factor method for damage identification in plate–type structures, *Mech Syst Signal Pr* 2012; **28**: 660–78.
41. Hajizadeh AR, Salajegheh E, Salajegheh J. 2–D Discrete wavelet–based crack detection using static and dynamic responses in plate structures. *Asian J Civ Eng* 2016; **17**(6): 713–35.
42. Pakrashi V, Basu B, O'Connor A. Structural damage detection and calibration using a wavelet–kurtosis technique, *Eng Struct* 2007; **29**(9): 2097–2108.
43. Basu B. Identification of stiffness degradation in structures using wavelet analysis, *Constr Build Mater* 2005; **19**(9): 713–21.
44. Bagheri A, Ghodrati Amiri G, Seyedrazzaghi SA. Vibration–based damage identification of plate structures via curvelet transform, *J Sound Vib* 2009; **327**: 593–603.
45. Hajizadeh AR, Salajegheh J, Salajegheh E. Performance evaluation of wavelet and curvelet transforms based–damage detection of crack types in plate structures, *Struct Eng Mech* 2016; **60**(4): 667–91.
46. Vafai S, Salajegheh E. Comparisons of wavelets and contourlets for vibration based damage identification in the plate structures, *Adv Struct Eng* 2019; **22**(1): 136943321882490.
47. Jahangir H, Khatibinia M, Kavousi M. Application of contourlet transform in damage localization and severity assessment of prestressed concrete slabs, *J Soft Comput Civ Eng* 2021; **5**(2): 39–67.
48. Jahangir H, Khatibinia M, Mokhtari Masinaei M. Damage detection in prestressed concrete slabs using wavelet analysis of vibration responses in the time domain, *J Rehabil Civ Eng* 2022; **10**(3): 37–63.
49. Vafai S, Salajegheh E. A comparative study of shearlet, wavelet, laplacian pyramid, curvelet, and contourlet transform to defect detection, *J Soft Comput Civ Eng* 2023; **7**(2): 1–42.
50. Burt PJ, Adelson EH. The laplacian pyramid as a compact image code, *IEEE T Commun* 1983; **31**(4): 532–40.
51. Do MN, Vetterli M. The contourlet transform: an efficient directional multi resolution image representation, *IEEE T Image Process* 2005; **14**: 2091–106.
52. Hinton E. Numerical methods and software for dynamic analysis of plates and shells. Swansea, Pineridge Press 1988.
53. The MathWorks, Inc. MATLAB the language of technical computing. <www.mathworks.com>, 2009.